Experimental permeability measurement of different reinforcement types for virtual permeability determination validation

BOUBAKER Mouadh[1,a] *, WIJAYA Willsen[2,b], CANTAREL Arthur[1,c],
DEBENEST Gérald[3,d], BICKERTON Simon[2,e]

[1] Institut Clément Ader (ICA), CNRS UMR 5312, University of Toulouse, IUT of Tarbes, UPS, France

[2] Centre for Advanced Materials Manufacturing and Design, Department of Mechanical Engineering, The University of Auckland, Auckland, New Zealand

[3] INPT, UPS, IMFT (Institut de Mécanique des Fluides de Toulouse), Université de Toulouse, Allée Camille Soula, 31400, Toulouse, France

[a] MOUADH.BOUBAKER@iut-tarbes.fr, [b] willsen.wijaya@auckland.ac.nz, [c] arthur.cantarel@iut-tarbes.fr, [d] gerald.debenest@toulouse-inp.fr, [e] s.bickerton@auckland.ac.nz

Keywords: Composites, Experimental Permeability, Virtual Permeability, CFD, Porous Media

Abstract. Permeability measurement of engineering textiles is a key step in preparing composites manufacturing processes. A radial flow experimental set-up is used in this work to characterize the unsaturated and saturated in-plane permeabilities of different types of textiles. In order to identify fabrics in which the dual-scale flow effect is stronger, comparisons are made between the measured saturating and saturated permeabilities. In parallel, the delayed tow saturation during the oil injection stage of the saturating measurement is observed visually. In addition, virtual permeability of porous media is studied using the numerical implementation of Darcy-Brinkman equation in a finite volume method (FVM) open-source software (OpenFOAM). A numerical method is proposed to determine the permeability of a given geometry at mesoscale. The method is used to determine the permeability of a realistic geometry acquired using an X-ray micro tomography (µCT) scanner and the results are compared to experimental values obtained with the proposed experimental set-up on the same plain weave textile.

Introduction

Composite materials are increasingly and widely applied in automobile, shipbuilding, aeronautics and aerospace applications. These materials are fabricated from fibrous reinforcements that can take the form of woven fabrics, non-crimp fabrics, knits, braids or random mats [1]. The fabrics are transformed into composite parts using different manufacturing processes. One of the most used and developed manufacturing methods is the Liquid Composite Molding (LCM) due to its various advantages, being low-cost, clean and more efficient than other methods. This fabrication process is based on the impregnation of a dry reinforcement with a low viscosity resin. During the impregnation step, the liquid resin flows through the channels of the reinforcement which can be considered as a porous medium. This flow is a key phenomenon in the modeling of the manufacturing process and has a significant effect on the quality of the final part. An important parameter to be considered at this step is the permeability of the preform, which quantifies the ability to be crossed by a fluid. The permeability influences the resin flow front advancement inside the pores and as a result it controls the mold filling time which is a crucial parameter of composite fabrication optimization.

In order to meet the growing demand for composites, different types of reinforcements are being developed with different properties and architectures. Therefore, an accurate and efficient method

to characterize these reinforcements is needed, errors in permeability prediction for example can lead to an inefficient process design and the appearance of defects in parts such as voids and dry spots.

In the scope of this paper, we are interested in characterizing the permeability of a given reinforcement. Different permeability determination methods can be found in the literature and can be classified into three main groups: analytical methods, experimental methods and numerical methods.

Different analytical models relate the permeability to the fibre volume fraction and are based on simplifying assumptions where the fibres are modeled as cylinders arranged in regularly ordered networks (quadratic and hexagonal) [2]. These models are based on idealistic assumptions and do not accurately represent the complexity of the real preforms, in addition they are only valid for a certain range of fibre volume fractions. Alternatively, many researchers used experimental procedures to measure the permeability of fibrous domains. These experiments give more accurate results but have the disadvantage of being time and material-consuming and labor-intensive since they involve many sensors, transducers and digital cameras [3]. Another drawback is the absence of a standard approach. Several international benchmark exercises [4-6] were launched in order to study the variation in the experimental measurements on different geometries (non-crimp and woven fabrics) and found a coefficient of variation of up to 44% for the woven fabric for example.

A promising alternative is the use of numerical methods which combine textile modeling and computational fluid dynamics techniques. The potential of numerical methods is increasing with the increasing computing capabilities. The virtual permeability prediction has many advantages like the ability to explore a large range of parameters efficiently without needing to reproduce the experiment or without using big equipment and generating large amounts of waste. With these advantages come some challenges from the complex structure of reinforcements like the geometrical variability and the dual-scale porosity. This dual-scale porosity makes it necessary to use multiscale approaches in order to predict virtual permeability since macro-scale models are not accurate enough and micro-scale models are not efficient and need too much information. The meso-scale models seem to give a good compromise between accuracy and efficiency.

The flow of resin in a fibrous network is usually considered as a creeping flow because high velocities cannot be achieved which results in low values of the Reynolds number. In this case, Darcy's law (Eq. 1) can be used to model the resin flow. Being based on experimental observations, this law is a phenomenological macroscopic model [7] which gives a relation between the volume-averaged velocity and the volume-averaged pressure gradient and is used to characterize porous media at the macro scale

$$u = -\frac{K}{\mu}\nabla P \qquad\qquad\qquad (1)$$

u is the volume averaged velocity, K is the permeability tensor of the reinforcement, μ is the viscosity of the fluid and P is the volume-averaged pressure.

In the first section of this paper, a 2D radial experimental procedure to determine the in-plane permeability tensor of different textiles will be presented. The experimental set-up was designed in order to measure the unsaturated (transient) and saturated (steady-state) permeability in a single run. Different types of textiles were explored and one of them was scanned using an X-ray μCT scanner [3] and a virtual permeability prediction method was applied on the 3D virtual geometry obtained. The results of the numerical simulation will be compared to the experimental ones at different fibre volume fractions in order to test the accuracy of the virtual permeability determination method.

Experimental set-up for the permeability characterisation of fibrous textiles

A 2D radial in-plane permeability determination experimental set-up (Fig. 1) developed at the Centre for Advanced Materials Manufacturing and Design CAMMD of The University of Auckland is used to determine the unsaturated and saturated permeability of 5 different E-glass fabrics: quad axial stitched fabric, twill weave fabric, 0/90 biaxial stitched fabric, unidirectional reinforcement and a plain weave fabric. The experimental facility including the different tools used and the details of the experimental procedure will be presented and the results and the key findings will be discussed.
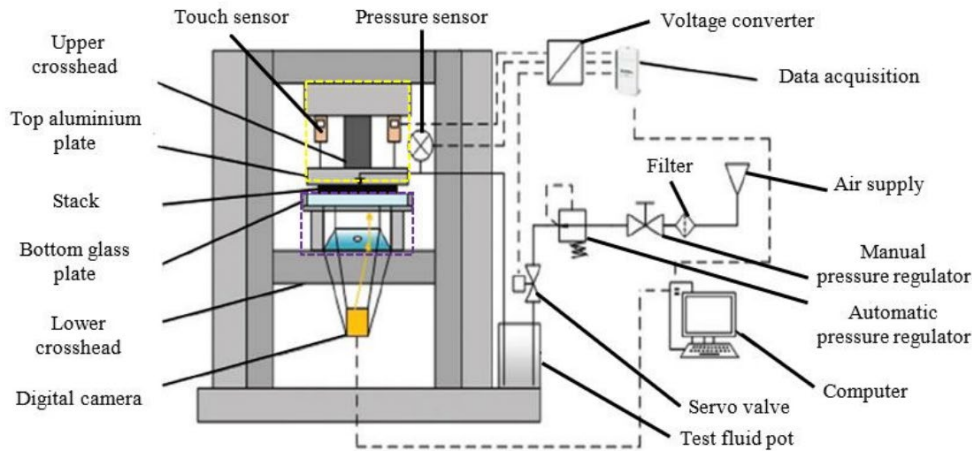

Fig. 1: Schematic representation of the experimental facility [3]

This setup was used by Zhang and Comas-Cardona et al. [8,9] to investigate transient permeability of Chopped Strand Mat (CSM) and other fabrics. This 2D in-plane radial flow permeability test rig has been developed over the years in order to efficiently characterize the in-plane permeability of fibrous textiles. This rig complies with the international standards found in the literature [4-6,10].

The experimental procedure involves the compaction between two rigid flat plates of the textile in order to get the desired fibre volume fraction through the control of the sample thickness. It involves also the injection of a test fluid via a circular port of a diameter of 15 mm located at the center of the sample, the test fluid used is a Newtonian Mobil DTE series HEAVY mineral oil ISO VG 100 which viscosity as a function of temperature was determined using a Parr Physica UDS200 rheometer. This mineral oil was used instead of a thermoset resin since the resin cure phase of the LCM does not affect the permeability measurements. The oil is supplied from an enclosed metallic pot driven by the pressurized air regulated by a FESTO proportional pressure controller. After being injected, the fluid will flow radially in the textile.

The radial flow technique was particularly chosen because of the relative simplicity of the setup compared to other techniques in addition to the ability to compute the complete in-plane unsaturated permeability tensor with a single test which minimizes the effort and the cost.

Experimental facility

The 2D radial testing facility is placed on an Instron 1186 Universal Testing Machine (UTM) that provides an accurate control of cavity thickness. The whole facility was assembled in an environmentally controlled (a constant temperature of 22°C) room to get consistent measurements. The sample is set between two plates: a glass lower plate made of 55 mm thick glass with a side length of 350 mm that allows flow front detection through optical monitoring in order to better understand the flow behavior, and a circular upper platen of a diameter of 250 mm and 30 mm thick that is aligned to the lower platen with a spherical alignment unit and a manufactured strain-

gauged compressive alignment specimen. Through these alignment tools, parallelism and uniform cavity thickness are achieved with a tolerance of 0.005 mm. These plates are designed in order to minimize deflection during the compaction step allowing a maximum deflection of 0.07 mm under an average compaction pressure of 2 MPa [9], the range of target thickness cavity was around 3mm which respects the ISO 4410 recommendations of target thickness being under 2%.

A Navitar (SV5C10 0238) digital camera was attached to the set-up via an L-bend with its lens pointing to an angled mirror of 45° with respect to the horizontal plate used to capture the flow front evolution during the test fluid infusion. Two touch sensors of type Mitutoyo IDU25 with 0.01 mm resolution were used to measure the distance between the parallel plates; they were attached to both sides of the top plate with their probe touching the upper surface of the bottom plate. The different measurement accuracies of the experimental facility are summarized in the following table:

Table 1: Measurement accuracies

Measurement	Accuracy
Sample mass	$\pm 0.01\ g$
Injected oil mass	$\pm 0.1\ g$
Cavity thickness	$\pm 0.005\ mm$
Fluid pressure	$\pm 1\%$

Experimental procedure

Using a dedicated circular cutting knife in a hydraulic press machine, circular stacks of 200 mm diameter of the fibrous textiles were prepared. A hole of 15 mm diameter was punched at the center of each sample in order to serve as an injection port. The mass of each sample was measured before starting the experiment using a digital balance. Then, the sample is placed on the bottom glass plate. The placement must be accurately centered in order to have a pure in-plane flow during the injection step. The position of this bottom plate is then monitored in order to achieve the target fibre volume fraction V_f given by equation (Eq. 2)

$$V_f = \frac{m}{\rho A h} \qquad (2)$$

with m the mass of the sample, ρ is the fibre density (characteristic of the used fabric), A the sample's planar area and h is the target compaction thickness.

The oil is then injected at a fixed nominal injection pressure of 50 kPa and the flow front progression is recorded as a series of images at the frequency of 1 Hz (Fig. 2).
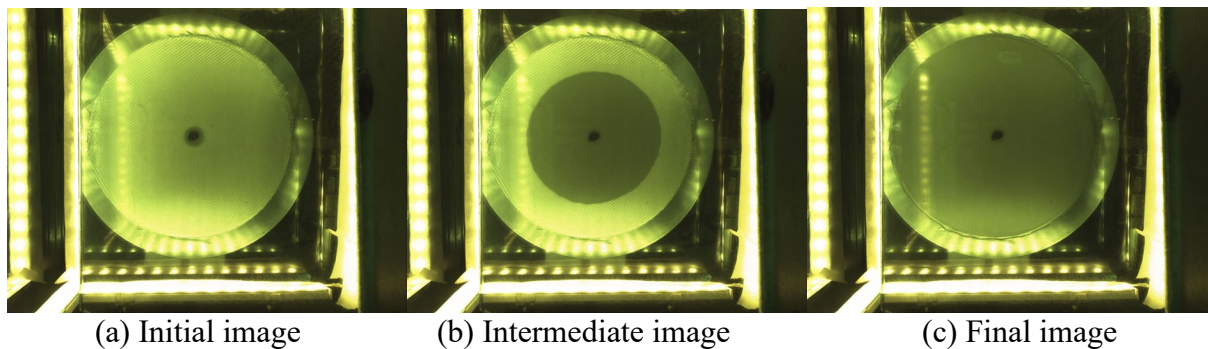

(a) Initial image   (b) Intermediate image   (c) Final image

Fig. 2: Flow front progression with time.

In addition to the flow front levels, other parameters need to be recorded during the experimental run in order to be used in the permeability computation using the formula given by

Weitzenbock et al. [11] in equations (Eq. 3 and Eq. 4). These parameters are the static inlet pressure measured by a pressure sensor located at the inlet and the oil temperature measured by a thermocouple in the pressure pot.

$$K_{11} = (a^2[2ln(\frac{a}{r_i}) - 1] + r_i^2)\frac{\mu(1-V_f)}{4tP} \qquad (3)$$

$$K_{22} = (b^2[2ln(\frac{b}{r_i}) - 1] + r_i^2)\frac{\mu(1-V_f)}{4tP} \qquad (4)$$

where K_{11} and K_{22} are respectively the major and minor in-plane principal permeability components, a and b are the major and minor radii of the fitted flow front ellipse, r_i is the radius of the injection hole, P the total pressure drop which can be approximated to the inlet pressure based on the atmospheric flow front pressure assumption, μ is the test oil viscosity deduced from the measured oil temperature and finally t is the time from the start of the injection. For each test, the permeability tensor is computed for each flow front image and plotted against the time steps. The reported permeability values are given by the average of the final one-third of the computed values to eliminate any flow stabilization effects at the start of the experiment. This setup also allows the prediction of isotropic saturated permeability. An additional quantity of oil is injected inside the sample after being fully saturated, which gives the saturated mass flow rate (by fitting a linear regression to the mass-time curve) and the steady-state permeability is deduced using Darcy's law through this equation (Eq. 5) [12]

$$K_{saturated} = \frac{Q \cdot \mu \cdot ln\left(\frac{r_0}{r_i}\right)}{2\pi \cdot \rho \cdot h \cdot P_{inj}} \qquad (5)$$

where Q is the mass flow rate, μ is the oil viscosity, r_0 is the sample's outer radius, r_i is the internal radius taken as the radius of the punched hole, ρ is the oil density, h is the cavity thickness and P_{inj} is the injection pressure.

Results

These experiments were carried out in order to observe the flow front advancement for different types of textiles used to manufacture composite parts and to quantify the difference between the transient and steady-state permeabilities of these textiles. The tests were carried out at three different fibre volume fractions V_f (0.5, 0.55 and 0.6) except for the twill-weave fabric for which only two V_f were targeted. The layers were oriented in a way that gives an isotropic flow in both directions (the flow fronts are almost circular) and the unsaturated permeability used for the comparison with the saturated value is an average of the values found for the principal directions $K_{unsat} = \sqrt{K_{11} \cdot K_{22}}$. The ratios K_{unsat}/K_{sat} were found to vary between 0.9 and 1.42 which lies in the range found in literature [13,14]. Researchers found ratios between 0.25, and 4 but for most of them [15,16] the ratio was around 1. Table 2 gives an overview of the results, each test was repeated 3 to 4 times and the relative standard deviation was between 3% and 16% which gives confidence on the repeatability of our results.

Table 2: Summary of the experimental results

Textile	V_f	$K_{sat}[10^{-10}m^2]$	$K_{unsat}[10^{-10}m^2]$	K_{unsat}/K_{sat}
E-glass Plain weave (800 g/m^2)	0.5	2.916 ± 0.19	3.16 ± 0.24	1.08
	0.55	1.12 ± 0.11	1.16 ± 0.14	1.04
	0.6	$0.482 + 0.06$	0.458 ± 0.054	0.95
0/90 Biaxial stitched fabric (825 g/m^2)	0.5	1.39 ± 0.2	1.6 ± 0.3	1.15
	0.55	0.672 ± 0.097	0.729 ± 0.11	1.08
	0.6	0.326 ± 0.044	0.34 ± 0.011	1.04
Quad Axial Stitched Fabric (851 g/m^2)	0.5	0.62 ± 0.026	0.649 ± 0.038	1.045
	0.55	0.27 ± 0.012	0.286 ± 0.007	1.05
	0.6	0.171 ± 0.016	0.177 ± 0.0178	1.03
Unidirectional reinforcement fabrics (850 g/m^2)	0.5	3.5 ± 0.22	4.97 ± 0.8	1.42
	0.55	1.91 ± 0.057	2.47 ± 0.097	1.29
	0.6	1.12 ± 0.16	1.33 ± 0.218	1.19
Twill weave (295 g/m^2)	0.5	0.398 ± 0.004	0.38 ± 0.045	0.96
	0.55	0.2 ± 0.022	0.183 ± 0.023	0.91

Observing the flow front advancement in the different textiles, it was noticed that the dual-scale effect, i.e. the difference of fluid velocity between the inter-tow and intra-tow space, is visible in the unidirectional (UD) reinforcement (Fig. 3(a)) and the Biaxial stitched fabrics (Fig. 3(b)), less visible for the plain weave textile (Fig. 3(c)), whereas, the flow front was nearly uniform for the twill weave and quad axial stitched fabrics and no impregnation delay was observed.
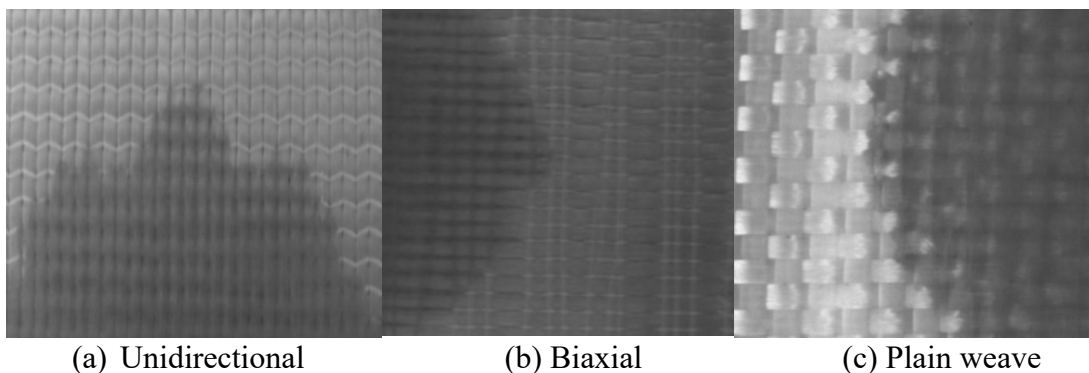

(a) Unidirectional   (b) Biaxial   (c) Plain weave

Fig. 3: Oil flow fronts during injection for different textiles.

Numerical method for permeability prediction

Numerical simulation is widely used at the component scale to simulate the LCM process but its usage for material characterization is not very well developed despite its increasing potential [17]. For complicated and realistic flow fields, numerical simulation is convenient. By imposing a

pressure gradient ΔP across the domain length L_{flow}, the steady state volumetric flow rate Q through a cross-section area A_{flow} can be numerically approximated by solving Stokes equation assuming creeping flow, i.e incompressible non-inertial characterized by a low Reynolds number, of a virtual incompressible Newtonian fluid of viscosity μ. The saturated permeability (capillary effects are not considered) is deduced using equation (Eq. 6) which is a simplification of Darcy's law (Eq. 1)

$$K = \frac{Q \cdot \mu \cdot L_{flow}}{A_{flow} \cdot \Delta P} \tag{6}$$

This numerical method is used to predict the saturated permeability of a fibrous reinforcement based on real images acquired from a 4 layers stack E-glass plain weave textile used in the previous experiment. The physical dimensions of the scanned specimen were $25.14\ mm \times 26.04\ mm$ with a variable height for each target fibre volume fraction (between $2.18\ mm$ and $3.28\ mm$). The voxel dimensions were 2012×2084 pixels in the weft and warp directions and a variable number of pixels in the through thickness direction (175 for the highest volume fraction 0.6 and 211 for the smallest one 0.5). The procedure of acquisition is described in detail by Wijaya et al. [18].

Single-scale flow
In this case, the tows are considered as solid impermeable zones and in order to optimize the simulation time and allocated computational resources, only the inter-tow space was meshed. The test fluid used has a viscosity of $\mu = 1\ mPa.s$ and a pressure gradient $\Delta P = p_{in} - p_{out} = 1000 - 100 = 900\ Pa$ is imposed between the inlet and the outlet.

The results of the numerical permeability in the weft direction compared to the experimental values for different fibre volume fractions are given in figure 4(a). The numerical method underestimates the experimental values for the different volume fractions which was expected since the flow inside the tows is neglected.
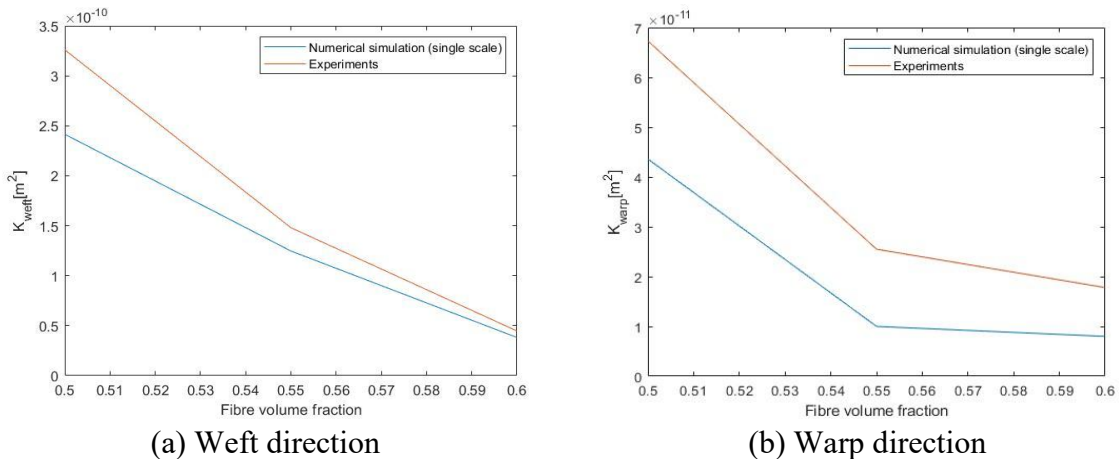

(a) Weft direction (b) Warp direction

Fig. 4: Comparison between the numerical simulation results and the experimental values.

We observe, in figure 4(b) a large scatter between the numerical simulation and the experimental results for the warp direction (60% for $V_f = 0.55$) compared to the weft direction (maximum of 25% for $V_f = 0.5$) which can be explained by the small size of the flow channels in the warp direction, therefore these narrow geometries are more difficult to be meshed and can be eventually removed if they are badly shaped. As a result, the numerical simulation underestimates the permeability in the warp direction. This problem can be solved if the flow inside the tows is taken into consideration.

Dual-scale flow

In this case, the tows are considered permeable and the fluid will flow both between and inside the tows. The same boundary conditions of the single-scale test are used. The permeability of the tows can be computed using the Gebart analytical model assuming hexagonal arrangement of fibers and using Gebart model (the fibers have a $12\ \mu m$ diameter) [2].

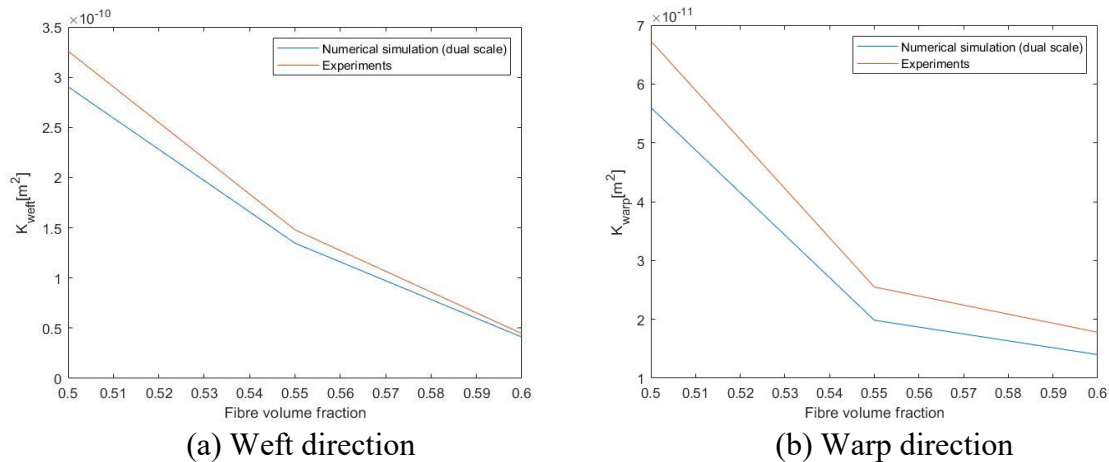(a) Weft direction   (b) Warp direction

Fig. 5: Comparison between the numerical simulation results and the experimental values considering dual scale.

As can be noticed in figure Fig. 5, the permeability values given by the numerical simulation considering porous tows are closer to the experimental values compared to single-scale tests which gives more confidence in the numerical method proposed. The deviation from the experimental values is reduced to 11% for $V_f = 0.5$ and 8% for $V_f = 0.6$ in the weft direction and it is around 20% in the warp direction which is a significant reduction compared to the single-scale case.

Conclusions

We used a 2D radial flow experimental set-up to investigate the discrepancy between the unsaturated and saturated permeability and to observe the flow front advancement during oil injection of different fabrics. The ratio between both permeabilities was between 0.9 and 1.42 which lies in the range found in the literature and was coherent with the flow front observations: the ratios were greater and different from 1 for the UD and biaxial textiles for example.

A numerical method for permeability prediction was used to estimate the permeability of the plain-weave textile which was already measured experimentally. A good agreement was found between the experimental and numerical values especially when the intra-tow flow is considered in the numerical simulation.

References

[1] V. Michaud, A Review of Non-saturated Resin Flow in Liquid Composite Moulding processes, Transp Porous Med, vol. 115, n 3, p. 581-601, déc. 2016. https://doi.org/10.1007/s11242-016-0629-7

[2] B. R. Gebart, « Permeability of Unidirectional Reinforcements for RTM », *Journal of Composite Materials*, vol. 26, nº 8, p. 1100-1133, août 1992. https://doi.org/10.1177/002199839202600802

[3] Willsen Wijaya. Permeability of 2D Woven Composite Textile Reinforcements: Textile Geometry and Compaction, and Flow Modelling. PhD thesis, 2020, The University of Auckland.

[4] D. May et al., In-plane permeability characterization of engineering textiles based on radial flow experiments: A benchmark exercise, Compos. Part A Appl. Sci. Manuf. 121 (2019). https://doi.org/10.1016/j.compositesa.2019.03.006

[5] N. Vernet et al, Experimental determination of the permeability of engineering textiles: Benchmark II, Compos. Part A Appl. Sci. Manuf. 61 (2014) 172–184. https://doi.org/10.1016/j.compositesa.2014.02.010

[6] R. Arbter et al. Experimental determination of the permeability of textiles: A benchmark exercise, Compos. Part A Appl. Sci. Manuf. 42 (2011) 1157–1168. https://doi.org/10.1016/j.compositesa.2011.04.021

[7] Darcy, Henry. "Les fontaines publiques de la ville de Dijon, Dalmont." Paris, France (1856).

[8] F. Zhang, S. Comas-Cardona, et C. Binetruy, Statistical modeling of in-plane permeability of non-woven random fibrous reinforcement, Composites Science and Technology, vol. 72, n 12, p. 1368-1379, 2012. https://doi.org/10.1016/j.compscitech.2012.05.008

[9] S. Comas-Cardona, B. Cosson, S. Bickerton, et C. Binetruy, An optically-based inverse method to measure in-plane permeability fields of fibrous reinforcements, Composites Part A: Applied Science and Manufacturing, vol. 57, p. 41-48, 2014. https://doi.org/10.1016/j.compositesa.2013.10.020

[10] Sousa Pedro, Lomov Stepan V., Ivens Jan, Hurdles and limitations for design of a radial permeameter conforming to the benchmark requirements. Frontiers in Materials, 9, 2022. https://doi.org/10.3389/fmats.2022.871235

[11] J. R. Weitzenbock, R. A. Shenoi, et P. A. Wilson, Radial flow permeability measurement. Part A: Theory, Composites Part A: Applied Science and Manufacturing, vol. 30, n 6, p. 781-796, 1999. https://doi.org/10.1016/S1359-835X(98)00183-3

[12] R. Pomeroy, S. Grove, J. Summerscales, Y. Wang, et A. Harper, Measurement of permeability of continuous filament mat glass–fibre reinforcements by saturated radial airflow, *Composites Part A: Applied Science and Manufacturing*, vol. 38, nº 5, p. 1439-1443, 2007. https://doi.org/10.1016/j.compositesa.2006.11.011

[13] K. M. Pillai, Modeling the Unsaturated Flow in Liquid Composite Molding Processes: A Review and Some Thoughts, *Journal of Composite Materials*, vol. 38, nº 23, p. 2097-2118, 2004. https://doi.org/10.1177/0021998304045585

[14] M. F. Foley et T. Gutowski, The effect of process variables on permeability in the flexible resin transfer molding (FRTM) process, p. 326-340, 1991.

[15] B. R. Gebart et P. Lidström, Measurement of in-plane permeability of anisotropic fiber reinforcements, *Polymer Composites*, vol. 17, nº 1, p. 43-51, 1996. https://doi.org/10.1002/pc.10589

[16] M. Pollard, Permeabilities of Fiber Mats Used in Resin Transfer Molding, 24th International SAMPE Technical Conference, pp. T408–T420, 1992.

[17] T. Schmidt, D. May, M. Duhovic, A. Widera, M. Humbert, et P. Mitschang, A combined experimental–numerical approach for permeability characterization of engineering textiles, Polymer Composites, vol. 42, n 7, p. 3363-3379, 2021. https://doi.org/10.1002/pc.26064

[18] W. Wijaya, M. A. Ali, R. Umer, K. A. Khan, P. A. Kelly, et S. Bickerton, An automatic methodology to CT-scans of 2D woven textile fabrics to structured finite element and voxel meshes, Composites Part A: Applied Science and Manufacturing, vol. 125, p. 105561, 2019. https://doi.org/10.1016/j.compositesa.2019.105561